

BROADBAND SPECTRAL-POLARIMETRIC BRDF SCAN SYSTEM AND DATA FOR SPACECRAFT MATERIALS

David L. Bowers, L. David Wellems

Applied Technology Associates 1300 Britt Street SE, Albuquerque, NM 87123-3353

Michael J. Duggin, William Glass, Leslie G. Vaughn

*Air Force Research Laboratory Space Vehicle Directorate 3550 Aberdeen Drive SE,
Kirtland AFB, NM 87117*

ABSTRACT

A broadband spectral-polarimetric Bidirectional Reflectance Distribution Function (BRDF) measurement system from 350nm to 2500nm with 1nm wavelength resolution is providing data for satellite radiance modeling and specifically for Michigan Tech's OCULUS-ASR space mission. The satellite has four deployable panels, which are covered with solar cells on one side, and are brightly colored on the other. BRDF data for the colored panels show interesting spectral features, including wavelength variability of first surface scatter, volumetric scatter and second surface scatter. Additional surface scatter data for other spacecraft materials including anodized aluminum, multilayer insulation (MLI) and solar cells is presented. The continuum nature of the data indicates that either dedicated BRDF models or a method for incorporating complex wavelength data into simulations will be needed for passive spectral radiance modeling and accurate spectral correlations.

1.0 INTRODUCTION

A major predictive radiometric model for space objects is the Time-domain Analysis Simulation for Advanced Tracking (TASAT) model. TASAT [1] ingests Bidirectional Reflectance Distribution Function (BRDF) parameters derived from BRDF measurements made at only a few wavelengths. Spectral interpolation of these parameters belies the complexity observed in our scan system. High resolution wavelength data from our scan system is being incorporated into TASAT allowing passive spectral radiance calculations or color band magnitude calculations to be made. Such calculations will be needed to obtain a better understanding of the dependence of multiband optical characteristics of OCULUS-ASR on solar phase angle.

BRDF measurements of diffuse looking homogeneous surfaces are the simplest to perform and are easiest to model. As surfaces become smoother, more heterogeneous, wrinkled, or layered, this situation becomes much more complicated. The OCULUS-ASR painted anodized materials were relatively easy to measure but the BRDFs will be difficult to model. Judgments whether to use texturing, or an average BRDF, or perhaps optical cross section (OCS) values, or whether to input experimental data without trying to make a surface scatter model must be made. This paper seeks to give an appreciation of the optical scatter physics from satellite materials and highlight the complexity required in modeling such materials. Complementary BRDF and OCS measurements, each with their own benefits and limitations, are used to provide insight into modeling complexities and help specify and interpret remote observations.

Mathematically, the BRDF is something of an idealized entity. Variations in spot size, source size or coherence, sample size, surface texture, mounting or material components often need to be considered before making a BRDF measurement. The measured BRDF represents angular convolutions of the source distribution and sensor angular field of view (FOV) with the ideal BRDF. In predicting surface radiance of wrinkled material multilayer insulation (MLI), a solar cell, a solar panel, or a mottled looking or weathered surface, analysts can be overly concerned with close-in appearances, using micro-area BRDFs, and surface texturing and many material components. A BRDF, average BRDF or OCS are all related and usage depends on end user requirements. For a flat surface of a known area an average BRDF and OCS may be related by Eq. 1, where *Area* is the viewed area of the object where θ , φ are view angles for a given illumination angle.

$$\langle BRDF(\theta, \varphi) \rangle = \frac{OCS(\theta, \varphi)}{\pi * Area} \quad (1)$$

Report Documentation Page

Form Approved
OMB No. 0704-0188

Public reporting burden for the collection of information is estimated to average 1 hour per response, including the time for reviewing instructions, searching existing data sources, gathering and maintaining the data needed, and completing and reviewing the collection of information. Send comments regarding this burden estimate or any other aspect of this collection of information, including suggestions for reducing this burden, to Washington Headquarters Services, Directorate for Information Operations and Reports, 1215 Jefferson Davis Highway, Suite 1204, Arlington VA 22202-4302. Respondents should be aware that notwithstanding any other provision of law, no person shall be subject to a penalty for failing to comply with a collection of information if it does not display a currently valid OMB control number.

1. REPORT DATE SEP 2011	2. REPORT TYPE	3. DATES COVERED 00-00-2011 to 00-00-2011			
4. TITLE AND SUBTITLE Broadband Spectral-Polarimetric BRDF Scan System and Data for Spacecraft Materials		5a. CONTRACT NUMBER			
		5b. GRANT NUMBER			
		5c. PROGRAM ELEMENT NUMBER			
6. AUTHOR(S)		5d. PROJECT NUMBER			
		5e. TASK NUMBER			
		5f. WORK UNIT NUMBER			
7. PERFORMING ORGANIZATION NAME(S) AND ADDRESS(ES) Air Force Research Laboratory, Space Vehicles Directorate, 3550 Aberdeen Dr SE, Kirtland AFB, NM, 87117		8. PERFORMING ORGANIZATION REPORT NUMBER			
9. SPONSORING/MONITORING AGENCY NAME(S) AND ADDRESS(ES)		10. SPONSOR/MONITOR'S ACRONYM(S)			
		11. SPONSOR/MONITOR'S REPORT NUMBER(S)			
12. DISTRIBUTION/AVAILABILITY STATEMENT Approved for public release; distribution unlimited					
13. SUPPLEMENTARY NOTES AMOS, Advanced Maui Optical and Space Surveillance Technologies Conference, 12-16 Sep 2011, Maui, HI.					
14. ABSTRACT A broadband spectral-polarimetric Bidirectional Reflectance Distribution Function (BRDF) measurement system from 350nm to 2500nm with 1nm wavelength resolution is providing data for satellite radiance modeling and specifically for Michigan Tech's OCULUS-ASR space mission. The satellite has four deployable panels, which are covered with solar cells on one side, and are brightly colored on the other. BRDF data for the colored panels show interesting spectral features, including wavelength variability of first surface scatter, volumetric scatter and second surface scatter. Additional surface scatter data for other spacecraft materials including anodized aluminum, multilayer insulation (MLI) and solar cells is presented. The continuum nature of the data indicates that either dedicated BRDF models or a method for incorporating complex wavelength data into simulations will be needed for passive spectral radiance modeling and accurate spectral correlations.					
15. SUBJECT TERMS					
16. SECURITY CLASSIFICATION OF:			17. LIMITATION OF ABSTRACT Same as Report (SAR)	18. NUMBER OF PAGES 9	19a. NAME OF RESPONSIBLE PERSON
a. REPORT unclassified	b. ABSTRACT unclassified	c. THIS PAGE unclassified			

Laser measurements are important and offer BRDFs with high angular fidelity. However, for smooth composite materials such as solar cells and mounting dependent materials such as Kapton, laser BRDFs may yield an unrealistic brightness baseline. For example, micro sampling on a localized area of smooth Kapton or a solar cell might yield peak BRDFs on the order of 100,000 (1/sr) or more and may not appropriately sample surface warping. Peak BRDF measurements may be limited by the angular divergence of the source and receiver FOV. If the receiver is not the limiting factor then the theoretical maximum BRDF is given by $1/\Delta_s$, where Δ_s is the solid angle of the source in steradians (sr). For rough samples, BRDFs measurements using either a laser or an incandescent source will be the same [2].

The theoretical maximum BRDF for a perfect reflecting ($R=1$) surface under solar illumination is 14,718 (1/sr). Ideally, for BRDFs that are to be used in passive radiance calculations, the source should have the angular diameter of the sun. In our scan system, both source and receiver limit the BRDFs to about 5000(1/sr) for an $R=1$ surface and using minimum source and receiver apertures. A way around this scan system limitation difficultly is to photograph the scatter pattern of the entire illuminated smooth surface reflecting on a movie screen. For the case of the solar cell, the cell was illuminated by a lab sphere source, which simulates the sun, and a flat glass reference with a known OCS value was measured simultaneously with the sample. Note that in the far field of the glass reference, the screen reference spot is circular and is independent of the reference shape. The scan system solar cell BRDF spectra, which are source and receiver limited, can then be appropriately scaled by the OCS profile. When scaling spectra care must be taken to ensure there are no spectral variations over the system angular convolution mask.

2.0 TYPES OF OPTICAL SCATTER MEASUREMENTS

This section describes BRDF scan system data and a complementary approach to BRDF measurements when the smooth surface BRDF exceeds the limit of the scan system. The materials measured are shown in the documentation photograph of Fig. 1 which shows a generic 1.5"x3" solar cell, generic 3" x 6" wrinkled and 2"x2" smooth Kapton and the 2"x2" OCULUS-ASR samples. For the solar cell and smooth Kapton, complementary or OCS measurements to the scan system data were required. For colored OCULUS-ASR samples, the measurements did not appear system limited, so scaling was unnecessary. In general, a case can be made for obtaining and using OCS measurements in modeling efforts.

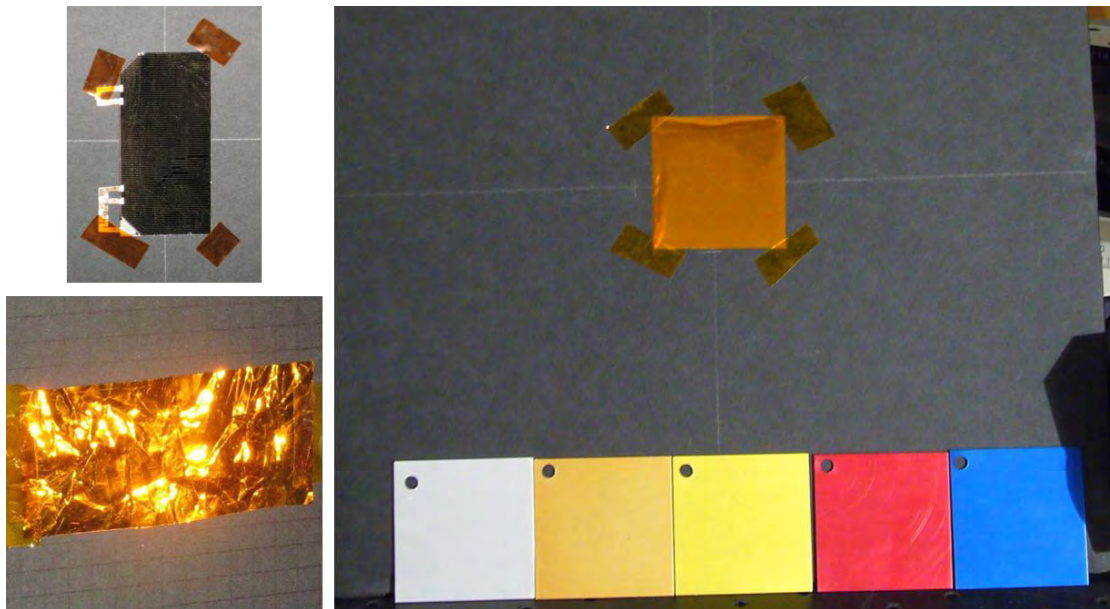


Fig. 1. Documentation photographs of a generic solar cell (upper left), generic wrinkled Kapton (lower left), generic smooth Kapton (upper right) and the OCULUS-ASR aluminum samples (lower right).

2.1 BRDF Capability

The BRDF scan system is centered on the ASD spectrometer. It uses a number of motors to accurately control the in-plane and out-of-plane target position, the in-plane source position and the source and receiver polarizer positions. The system uses a high power broadband light source to provide continuous (1 nm steps) spectral-polarimetric BRDF data from 350nm to 2500nm at each position. Positioning limitations are shown in the top view scan system schematic of Fig. 2. The scans run unattended with a user defined 'motor position' file. Typical scans include fixed angle of incidence (AOI) multiple angles of view (AOV) and 'scissor' scans where the AOI and AOV are equal and vary from near normal to near glancing.

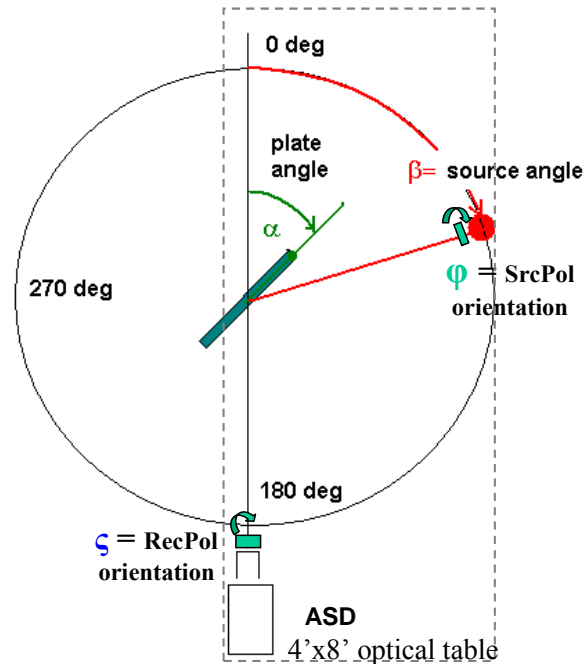


Fig. 2. Top view schematic of the broadband spectral-polarimetric BRDF scan system.

Scan system output visualization and data files include

- full spectral information at a fixed AOI AOV,
- full spatial information at a fixed wavelength and
- full spectral-spatial 3D data,

for

- s-polarized to s-polarized (SS),
- s-polarized to p-polarized (SP),
- p-polarized to s-polarized (PS),
- p-polarized to p-polarized (PP) and
- un-polarized to un-polarized (UU) which is one-half the sum of the cross and co-polarized components.

Peak BRDF measurements are driven by the angular divergence of the source and receiver. A standard configuration for our system uses a 1" source aperture ~30" from the target and a 2 degree field of view (FOV) receiving lens ~40" from the target. The BRDF scan system sampling diameter is typically about 3.3 cm. Source and receiver distances and aperture sizes may be varied to allow for higher peak BRDF measurements. For smooth materials an OCS measurement of the sample at discrete wavelengths is obtained and the BRDF UU data is scaled using Eq. 1. The OCS measurement also provides a 2D angular distribution for a fixed geometry at discrete wavelengths. Details of the OCS measurement technique are described next.

2.2 OCS Capability

OCS measurements are important for capturing macro light scatter from composite and textured materials such as solar cells, solar panels, MLIs and entire satellites. If the surfaces are fairly flat these measurements may be related to the BRDF through Eq. 1 and used to scale the BRDF scan system data. One of the methods we have developed captures the specular 2D angular distribution of scatter from an object for a fixed AOI and AOV in a single image. The OCS measurement is not limited by the receiver FOV and illumination uses a broadband source with the proper solar divergence. An advantage of the OCS measurements is that the peak specular values can be identified in the scattered pattern image. In scan system measurements peak values depend on alignment, mounting and sample flatness. Additionally, OCS at single angular locations can be determined by imaging the sample and reference directly. The advantage of this, direct view, method is more signal and surface warping can be seen but the data is limited to a single angular location in the glint field.

OCS measurements of the solar cell and smooth Kapton samples were obtained to scale the UU scan system BRDF data. In the case of the solar cell, the cell was completely illuminated by a distance lab sphere and reflections from the cover glass, cell, backing and metal wires are folded into a single average BRDF or OCS measurement. A thermo electric cooled lowlight camera with a variety of 10nm filters with center wavelengths across 400nm to 900nm were used to photograph the scatter pattern. For the case of the smooth Kapton samples, the BRDF magnitudes are mounting and sample dependent.

The level of detail and fidelity required of measurements and modeling is application specific. The micro and macro views of BRDF and OCS measurements complement one another and ease measurement limitations present in each method. The OCS is used to anchor system limited BRDF and shows the macro structure of composite surfaces but is limited in AOI and AOV geometries. The BRDF captures many AOI and AOV geometries but is magnitude limited for smooth surfaces.

3.0 OPTICAL SCATTER MEASUREMENTS OF OCULUS-ASR COUPON SAMPLES

Subsets of the BRDF data for the yellow anodized aluminum OCULUS-ASR sample are presented. The anodized aluminum coupons have complicated spectral shapes indicating both first surface and lower surface reflections as well as absorption and scatter from the colored anodizing film. Cross-polarized BRDF data on household paints is most associated with volume scatter from pigments, but colored anodized coupon data indicated that co-polarized reflection contains pigment spectral information as well. This data is needed for improving BRDF models of anodized surfaces and shows that both first and back surface reflection need to be included.

Fig. 3 shows the 60° AOI, 0° AOV off-specular and 60° AOI, 60° AOV specular wavelength data for the yellow coupon sample. From the off-specular data, the SS and PP appear to have reflective surface contribution and volume scatter components and the SP and PS are pure volume scatter components. From the specular data, PP is still carrying color information at (60°, 60°), showing that a sensor polarizer could bring out the color information. Notice that the PP values on the right plot are much larger than the PS and SP volumetric or multiply scattered components. Because the color spectrum is present in the PP rays, these have penetrated the film and are being reflected at an internal film/metal interface and are not being fully depolarized by pigments. Were the film layer fully depolarizing, the PP would have a value similar to the cross polarized components. The SS on the right plot is nearly pure first surface reflection, basically spectrally neutral, and shows the surface smoothness with respect to a wavelength increase. An elaborate surface layer scatter model is needed to explain these results.

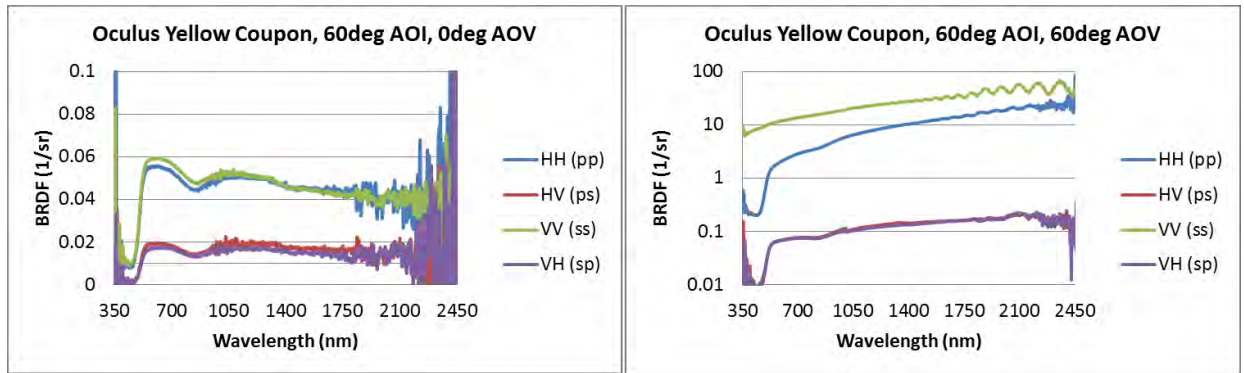


Fig. 3. 60° AOI off-specular and specular wavelength data for yellow coupon sample.

Full angle data for any one of the 2,250 wavelengths across the measured 350nm to 2500nm spectral region may be displayed. Full angle data at 525nm for the 30° and 60° AOI scans is shown in Fig. 4. From the 30° AOI data in this figure, SS and PP have reflective surface contribution and SP and PS are volume scatter components. The above comments hold for the blue and red coupon data.

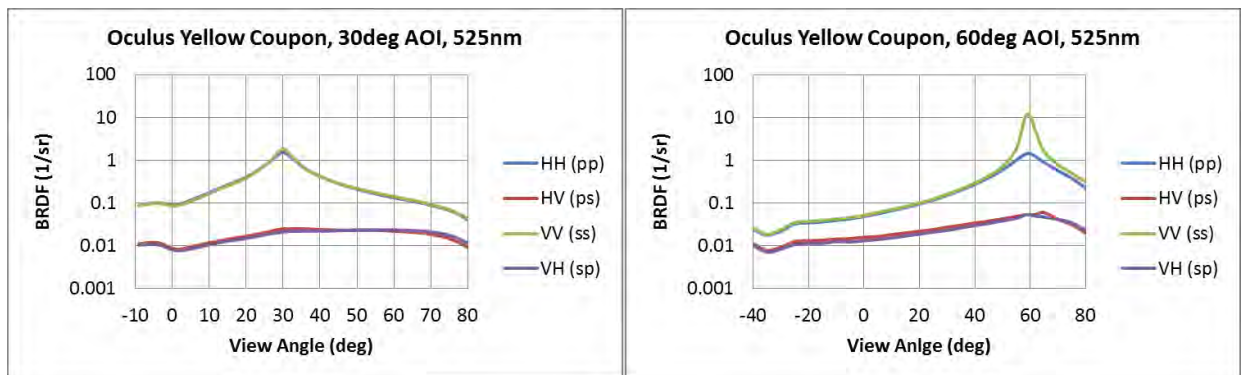


Fig. 4. 525nm 30° and 60° AOI angle data for the yellow coupon sample.

A comparison of Fig. 5 with Fig. 3 further highlights the contributions from the bare aluminum subsurface and the colored pigment surface. Fig. 3 is seen to be a combination of the Fig. 5 bare aluminum scatter and the yellow colored pigment scatter.

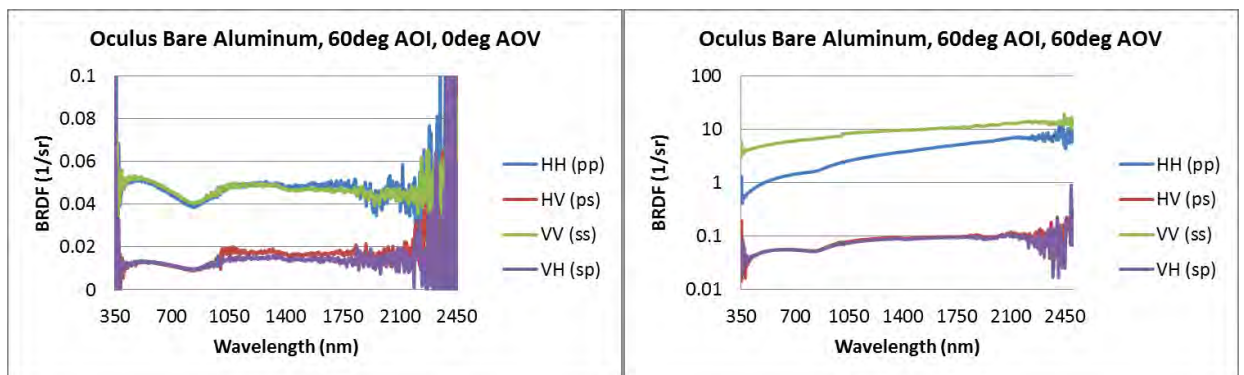


Fig. 5. 60° AOI off-specular and specular wavelength data for bare aluminum coupon sample.

4.0 OPTICAL SCATTER MEASUREMENTS OF SOLAR CELL AND KAPTON SAMPLES

In this section, BRDF scan system data for the generic solar cell and Kapton samples are scaled based on OCS profile measurements. High resolution angular OCS measurements described in section 2.2 were made at several

discrete wavelengths and shown to overlay the continuous scan system spectra, thus the scan system spectra is not being altered by the inherent spatial or angular convolution in the measurements. This scaling is depicted in Fig. 6 which shows UU scaled and un-scaled scan system data and the discrete filter and continuous spectra overlay.

Fig. 7 shows the 2D angular OCS mapping on the left and a line profile through the pattern on the right. For the OCS measurements the source angular diameter matched that of the sun. In the intensity image the glass reference pattern is on the left and the solar cell pattern is on the right. The peak OCS value at 690nm is near 11m^2 and the angular width is 0.6° . Corroborating direct view OCS data was also obtained. The peak OCS value was used to calculate an average BRDF which was used to determine a scale factor for the specular scan system BRDFs.

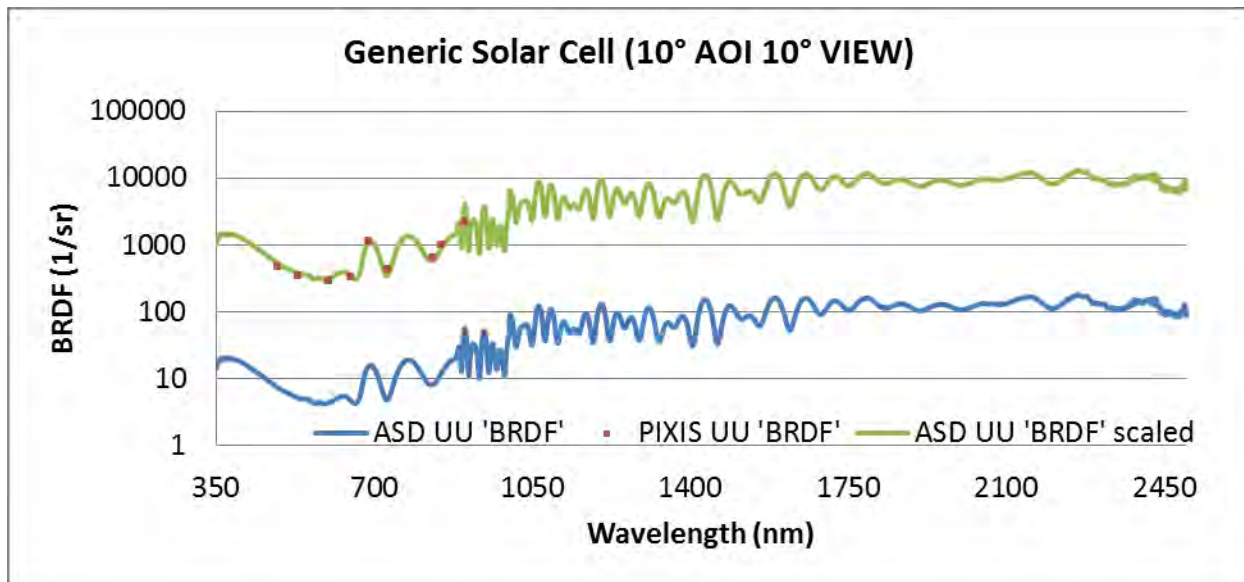


Fig. 6. Passive solar cell BRDF for passive radiance predictions.

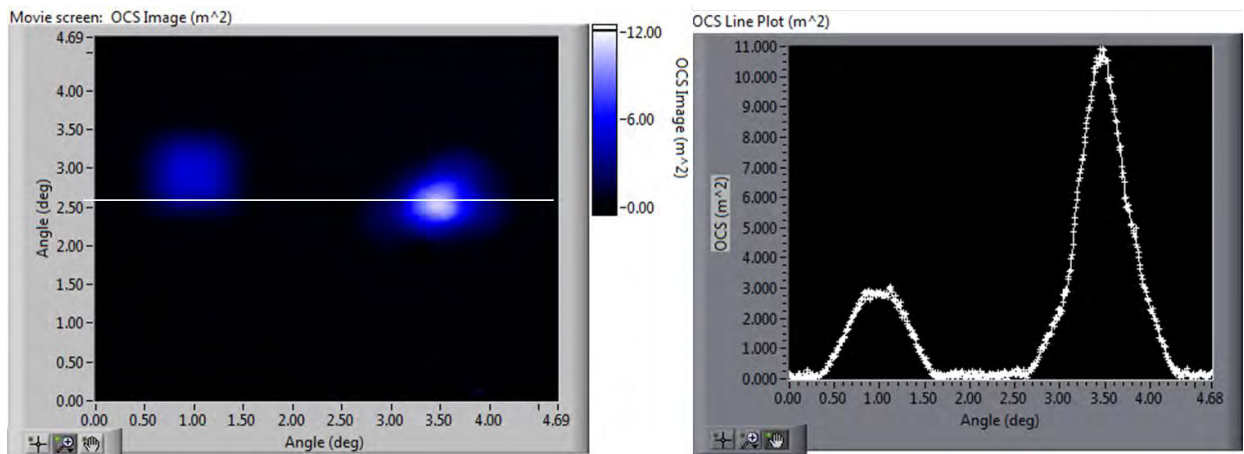


Fig. 7. 2D OCS reflective pattern of 2"x2" glass reference and 1.5"x3" solar cell, and corresponding line profile.

Fig. 8 shows solar cell UU BRDF data at off specular ($\text{AOI}=45^\circ$, $\text{AOV}=50^\circ$) and specular ($\text{AOI}=45^\circ$, $\text{AOV}=45^\circ$) geometries. At the off specular geometry a more neutral spectra associated with metal wire reflectance and at the specular geometry a reflectance spectra associated with semiconductor layers is evident. For comparisons, the off-specular data has been multiplied by 1000.

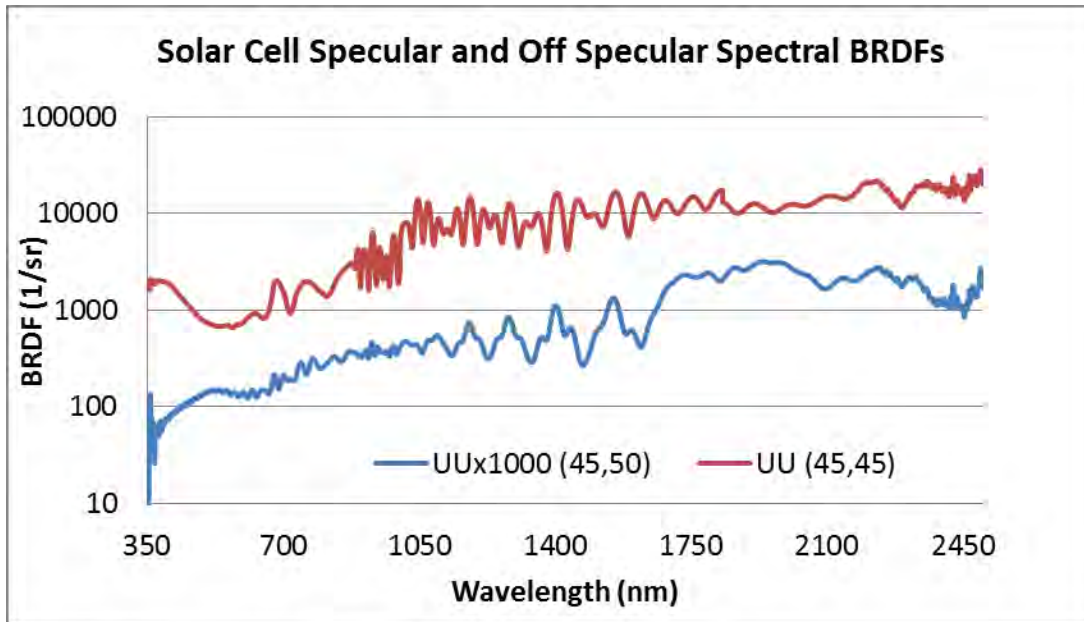


Fig. 8. Passive solar cell off-specular and specular BRDFs showing different surfaces dominating the spectra.

Passive BRDFs for smooth Kapton are shown in Fig. 9. Note the remarkable wavelength dependent birefringence as exhibited by the cross polarized components. The UU Kapton spectra, is a smooth monotonic spectra and does not show the spectral oscillations evident in each of the components. The birefringence depends on mounting azimuth. Modeling the polarimetric components would be extremely difficult and simple curve fitting to the UU data would be the best method for predicting passive radiance.

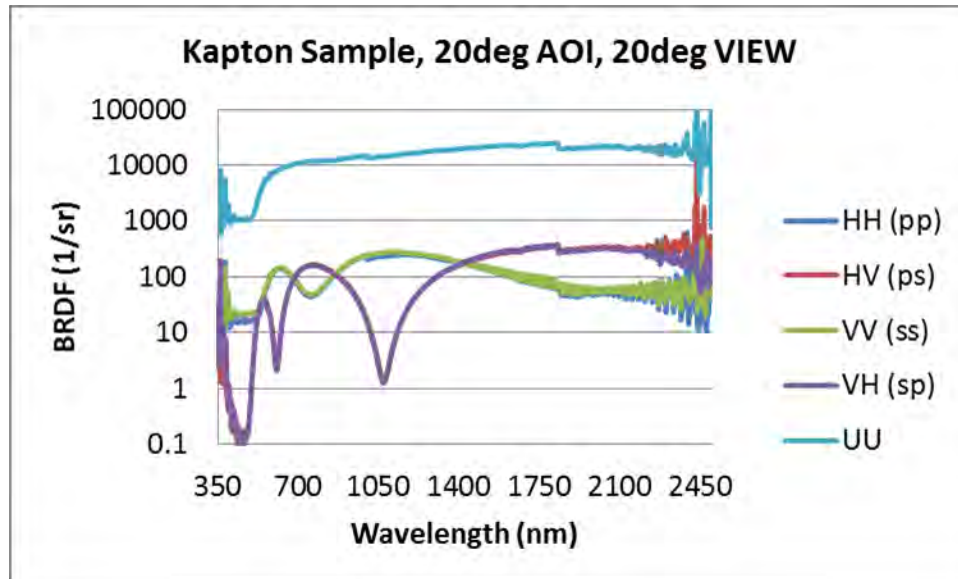


Fig. 9. Smooth Kapton BRDFs for passive radiance predictions.

5.0 DATA USE

The polarimetric BRDF data shows complex scattering processes. These data sets are necessary for understanding surface scatter physics and modeling purposes. The data sets may be used to specify which observational pass bands will distinguish between materials or for spectral correlation studies.

5.1 Illustrative Study for Attitude Determination from Spectra

Part of the OCULUS-ASR mission is to study the relationship between spectral radiance and solar phase angle. For example, the spectral angles between different BRDF data and ground based spectra, $Obs(\lambda)$, could be determined,

$$SA_i = \arccos \left(\frac{\sum_{\lambda} Obs(\lambda) * (Fil(\lambda) * BRDF_i(\lambda) * Sun(\lambda) * Cal(\lambda))}{(\sum_{\lambda} Obs^2(\lambda))^{\frac{1}{2}} (\sum_{\lambda} Fil^2(\lambda) * BRDF_i^2(\lambda) * Sun^2(\lambda) * Cal^2(\lambda))^{\frac{1}{2}}} \right) \quad (2)$$

The spectral angle, SA_i would be based on the filter used and calibration method, wavelength integration range and so forth. $Cal(\lambda)$ is a wavelength dependent factor that may come from using a standard reference star such as Vega, and $Fil(\lambda)$ would be the spectral transmission of observation filter, e.g., Johnson filter. From these correlation angles, the attitude or dominant reflecting materials could be determined. The closer the spectral angle is to 0° the more prominent that material in the measured return. Two simple illustrative examples are given in tables 1 and 2 where the filter, sun and calibration terms of Eq. 2 are not included. In table 1 the spectral angle in degrees is computed coupon color to coupon color for a single geometry. In table 2 the spectral angle in degrees is computed angle to angle for a single color coupon. In table 2 the AOI is constant at 30° and the AOV is varied. The spectral angle in degrees between the BRDF UU data at 30° AOV is computed for different AOVs. A rotatable polarizer could improve spectral correlation at larger phase angles by suppressing neutral 1st surface SS reflection. The decreasing correlation is a consequence of increasing spectrally neutral surface scatter as shown in [3].

Table 1. Spectral angle in degrees between color coupon samples for 30° AOI, 30° AOV UU BRDFs.

Coupon Samples	Yellow	Blue	Red
Yellow	0.0°	24.5°	11.8°
Blue	24.5°	0.0°	25.2°
Red	11.8°	25.2°	0.0°

Table 2. Spectral angle in degrees between yellow coupon sample at 30° AOI and different view angle.

Angle of View	55°	45°	40°	35°	30°
30°	12.9°	10.2°	7.3°	2.37°	0.0°

5.2 BRDF to Filter Photometry Data Base

A BRDF data base is necessary for material identification or discrimination. Depending on the fidelity of the surface scatter model and/or the view illumination geometry, either a BRDF model or BRDF data can be used for predictive correlation with remote observations. For OCULUS-ASR satellite coupons, the latter is the best approach in that an accurate layered surface scatter model for anodized paints has not been developed. Anodized paints are thought to be more resilient to space weathering and the BRDF data presented could prove useful in other analysis. High resolution (1nm) BRDF laboratory data may be used to predict color magnitudes that are typical of remote observations. Rather than inverting telescope measurements into unit spectral irradiance data for a correlation, the forward mathematical process of converting BRDF data into a predicted telescope observation is more desirable because the calibration method and filter bandwidth can be directly folded into such a process.

6.0 CONCLUSIONS

BRDF coupon data for different spacecraft materials has been presented. When surfaces are smooth scan system data is source or receiver limited and a methodology for evaluating BRDFs has been presented. The measured BRDFs are to be used for passive radiance predictions. The complexity of the BRDF data in this paper shows that elaborate surface scatter physics is needed for modeling, and perhaps accurate models may never be developed. For material B-V or color indices prediction and in the absence of accurate spectral BRDF models, a database of measured high resolution BRDFs of key materials is needed. This high resolution spectral data will help specify observatory filters and bandwidths that best discriminate materials and help verify and interpret remote observations

[4]. Illustrative spectral correlation calculations were performed for OCULUS-ASR coupon data. These types of calculations will be needed for surface normal or attitude determination.

Acknowledgement

We wish to thank Michigan Technical Institute for providing coupon samples of their satellite.

7.0 REFERENCES

1. Riker, J.F., Roark, J.T., Mikolajczak, D.F., Stogsdill, S.E., Walter, R.E., Brunson, R.L., Crockett, G.A., and O'Neil, B.D., *Satellite Imaging Experiment Tracking Simulation Results*, SPIE vol. 2221, 235-247 (1994).
2. Wellems, L.D. and Bowers, D.L, *Laboratory Imaging of Satellites and Orbital Appearance Estimation*, AMOS 2007 Conference; September 12-15, 2007.
3. Wellems, L.D. and Bowers, D.L, *Improved Hyperspectral Imagery Using Diffuse Illumination or a Polarizer*, Proc. SPIE Vol. 7065, 2008.
4. Payne, T.E. et al, *Color Photometry of Geosynchronous Satellites Using the SILC Filters*, Proc. SPIE Vol. 4490, 2001.